



Influence of cooling conditions on microstructure and mechanical property of Sn-0.3Ag-0.7Cu lead-free solder

Prajak JATTAKUL¹, Tavee MADSA², Piyawan SUNASUAN², and Niwat MOOKAM^{3,*}

¹ Department of Industrial Engineering, School of Engineering, King Mongkut's Institute of Technology Ladkrabang, Chalongkrung Road, Ladkrabang, Bangkok, 10520, Thailand

² Department of Industrial Engineering Technology, Faculty of Industry and Technology, Rajamangala University of Technology Rattanakosin Wang Klai Kangwon Campus, Prachuapkhirikhan 77110, Thailand

³ Department of Industrial and Production Engineering, Faculty of Industry and Technology, Rajamangala University of Technology Rattanakosin Wang Klai Kangwon Campus, Prachuapkhirikhan 77110, Thailand

*Corresponding author e-mail: niwat.moo@rmutr.ac.th

Received date:

16 February 2021

Revised date

8 April 2021

Accepted date:

16 April 2021

Keywords:

Sn-0.3Ag-0.7Cu solder;
Cooling conditions;
Microstructure;
Mechanical property

Abstract

This research has investigated the influence of cooling conditions on the microstructure and mechanical properties i.e., tensile strength and microhardness of Sn-0.3Ag-0.7Cu lead-free solder. In the experiments, casting was performed at 300°C with comparison between copper and stainless steel molds under slow and fast cooled conditions. X-ray diffractometer confirmed the presence of Cu₆Sn₅ and Ag₃Sn phases in the solder matrix. Lead-free solder solidified under slow cooled conditions exhibited β-Sn matrix with larger grain growth as compared to the fast cooled solder. The eutectic area of intermetallic compound (IMC) was found to increase with cooling rate. The tensile strength of slow cooled solder was greater than fast cooled solder for both molds. In addition, the microhardness of the solder was also influenced by cooling rate. The dimples size of fracture surface was decreased by higher cooling rate. A greater eutectic area of the Cu₆Sn₅ and Ag₃Sn phases of initial β-Sn matrix lead to lower values of the mechanical property from fast cooled conditions.

1. Introduction

The traditional lead-containing solders e.g., Sn-40Pb and Sn-37Pb are being replaced by the binary and ternary lead-free solder [1,2]. Mainly due to lead and lead-containing compounds which are toxic substances causing detrimental effects on the environment [3,4]. Furthermore, growing environmental concerns and related laws and regulations evolve the Restriction of Hazardous Substances (RoHS). This directive has contributed to the development of many lead-free solders to replace the lead-containing solders [5-7]. The ternary solder system is the most widely used lead-free solder in the industry, composed of Sn-Ag-Cu (SAC), this solder provides good solderability, high electrical conductivity, and a better mechanical property compared to Sn-Pb solder [7,8]. It is well known that SAC solders have a melting point higher than that of the eutectic SnPb solders [9]. Thus, high melting temperature will increase the soldering temperature which may cause thermal damage of the substrate and electronics devices. Moreover, the SAC solder is predisposed to the formation of multiple intermetallic phases due to the reaction of Sn, Ag, and Cu atoms in solder or diffusion between solder and substrate [10,11]. However, the presence of the intermetallic phases has been linked to brittleness and adversely altering the mechanical properties and reliability of solder joints [12]. In addition, the primary failure mode of solder was the brittle failure through intermetallic phase [13].

The SAC solders have two groups, a low and high-Ag lead-free solder. From literature, the Ag content affects the Ag₃Sn and Cu₆Sn₅ intermetallic compound (IMC) precipitate. In SAC 305 and SAC 405 solder alloys with high-Ag lead-free solder, the amount of Ag₃Sn and Cu₆Sn₅ IMCs increases as the Ag content increases and become distributed in a Sn-rich matrix [11]. Higher concentrations of Ag₃Sn causes a high tensile strength and a low elongation, but the moderate concentration of Ag₃Sn with another type of IMC (Cu₃Sn) causes the opposite action [8]. However, Gumaan *et al.* [14] reported that the tensile strength and yield strength decreased with increasing Ag₃Sn phase. Large areas of Ag₃Sn reduce the reliability of the solder, while faster cooling rates reduce the amount of Ag₃Sn phase [14]. This result concurred with Sundelin *et al.* [15] who found that slower cooling rates increased dispersion of Ag₃Sn in most SAC solders including SAC 305, SAC 387 and SAC 405. Lee and Huang [16] reported that tensile strength and hardness of SAC 305 solder increased at faster cooling rates due to the formation of a fine-grained primary Sn-rich phase surrounded by a fine eutectic structure. Yahaya *et al.* [17] documented the presence of Ag₃Sn and Cu₆Sn₅ phases, with faster solder cooling rates showing the highest hardness values due to phase refinement. The microstructure and mechanical properties of solder alloys are greatly influenced by cooling conditions that affect their reliability [16,17]. Refined grains ensure that the internal structure of solder joints is compact and can effectively resist external

pressure, thereby improving reliability [18]. Low temperature lead-free solders are widely used in industry because they reduce heat damage to electronic devices and boards. An attractive alternative to the Sn-0.3Ag-0.7Cu (SAC0307) solder is an improved version as a low melting temperature, low-cost solder by doping only a small amount of Ag. IMC quantity is also minimal due to low Ag concentration, while the Ag_3Sn and Cu_6Sn_5 phases occur as small rounded particles distributed in the microstructure [10]. Low Ag solder alloys often experience ductile failure through bulk solder [13].

Low silver alloys typically show two distinct melting phases as a low temperature melting phase corresponding to SnAg eutectic, and a high temperature phase corresponding to SnCu eutectic melting around 228°C [19]. However, the microstructure and mechanical properties of solder in low-Ag SAC systems are not concisely detailed in the literature, with limited reports concerning their intermetallic compound formation and microstructure and mechanical properties. Thus, the effects of cooling conditions on intermetallic compound formation and mechanical properties of SAC0307 lead-free solder were investigated. Results will provide useful information to better control the microstructure and mechanical properties of low-Ag SAC lead-free solder.

2. Experimental

Sn-0.3Ag-0.7Cu lead-free solder was used in this experiment. The solidus and liquidus temperature of solder were about 217°C and 226°C, respectively. Prior to casting, the solder bar was melted at 300°C, the liquid solder was cast in either copper or stainless steel molds in an electrical furnace for comparison. The casting samples were subsequently cooled with different conditions, i.e. furnace (slow

cooled) and air (fast cooled). After casting, samples were cut, mounted, and polished respectively. The polishing was performed with a series of silicon carbide grit paper at 600, 800, 1000 to 2000 grit, and finally with Al_2O_3 powders at 0.3 μm to 0.1 μm . Lastly, the samples were etched using Ar ion beam (IBM, Hitachi, IM 4000 Plus).

Optical microscope (OM, Olympus, BX 60 M) was first employed to examine the grain microstructures. The grain size numbers were obtained using an image analysis software program, in accordance with the ASTM E 1382 standard. Scanning electron microscopy (SEM, Jeol; JSM-5800LV) was then used to verify the microstructure and fracture surface. An energy dispersive spectroscopy (EDS, OXFORD INSTRUMENTS, X-Max) was then used to determine the chemical compositions of the intermetallic phases. An X-ray diffractometer (XRD, Bruker D8 Discover) was used to identify the crystalline structure of phases.

The tensile test specimens were milled using CNC milling machine (Emco model PC Turn 50), with the dimensions and geometry determined in accordance to the ASTM E 1382 standard. A universal testing machine (Zwick, Z020) was used to investigate the tensile strength of the samples and carried out at room temperature with a crosshead speed of 1.0 $\text{mm}\cdot\text{min}^{-1}$. Finally, the microhardness was measured with a vickers indenter tester (Wilson, Tukon 1102) with a load of 0.2 kg and a loading time of 10 s.

3. Results and discussion

3.1 Microstructure

The microstructure of solder samples with the different casting conditions is illustrated in Figure 1. The Sn-rich phase as represented

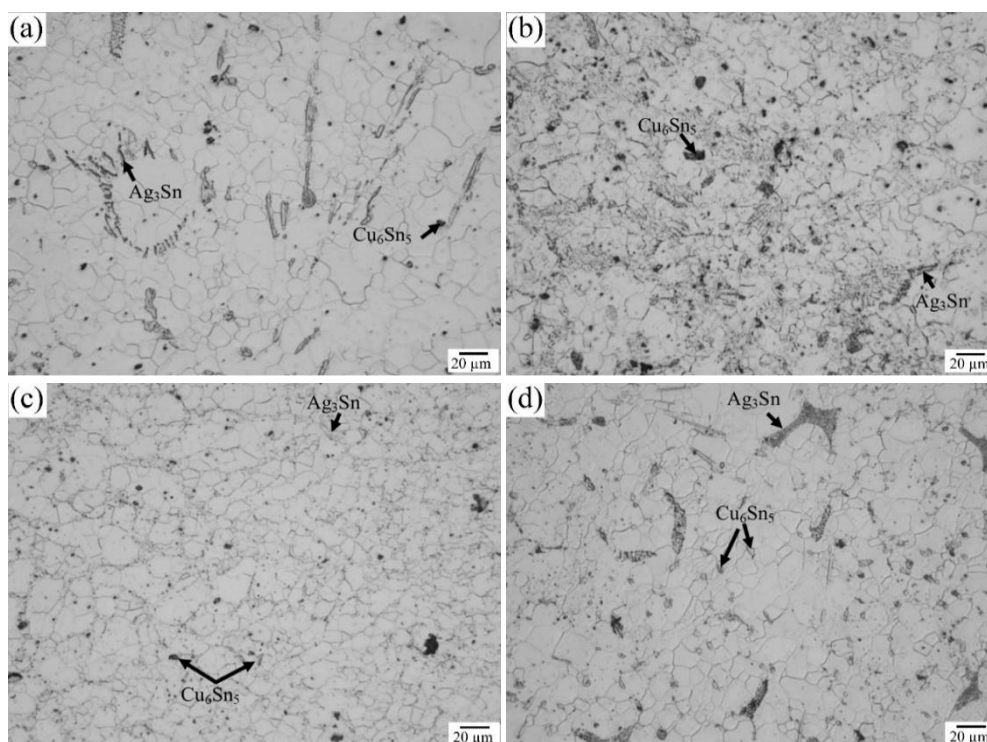


Figure 1. Optical microstructure of samples with difference condition casting: (a) copper mold with slow cooled (b) copper mold with fast cooled (c) stainless steel mold with slow cooled and (d) stainless steel mold with fast cooled.

by the light area with the dark area represent the intermetallic phases. As illustrated in Figure 1 (a)-(d), Sn-rich phase is the basic microstructure of Sn-3.0Ag-0.7Cu solder [20]. Nevertheless, the intermetallic particles were situated at the grain boundaries and with non-uniform distribution in the Sn-rich phase. The intermetallic phases of all samples comprised of Cu₆Sn₅ and Ag₃Sn. The EDS and elemental maps analysis indicated Sn-rich phase, Cu₆Sn₅ and Ag₃Sn as displayed in Figures 2 and Figure 3, respectively. XRD analysis was shown in Figure 4. The crystal structure, lattice parameters of Sn, Ag, Cu, and intermetallic phases were shown in Table 1. The crystal structure of Ag₃Sn found in this study was orthorhombic. Two types of Cu₆Sn₅ crystal structure found in solder matrix were hexagonal, and monoclinic. This indicated that monoclinic was found in the cast specimens, because the hexagonal have enough time to transform to monoclinic.

The microstructure of the alloy showed the Cu₆Sn₅ + Ag₃Sn network is formed in their eutectic region with large primary Ag₃Sn plate. The microstructure of the solder from copper and stainless steel casts is illustrated in Figure 5 and Figure 6, respectively. Samples cast with a copper mold show formation of the eutectic region is reduced by slower cooling rate. In addition, both Cu₆Sn₅ and Ag₃Sn phases were dense within the Sn-rich phase when fast cooled.

The microstructure of both molds show a significance difference. Compared to the copper mold, the cast with stainless steel mold depicts the cellular structure of intermetallic phase formation and IMCs particles separated along the grain boundary in the slow cooled solder, Figure 6. Thus, the IMC start to separate at the grain boundary due to a reduced nucleation energy [21]. In the fast cooled condition, an increase in the eutectic region is found. Thus, fast cooling promotes the formation of eutectic region.

However, solder alloy solidified in stainless steel mold has more uniform distribution with a smaller size of intermetallic particles. The cooling rate in microstructure increases with cooling media copper > stainless steel and air > furnace cooling [8]. Based on the cooling state, the type of intermetallic compound formation were similar. For all condition, microstructure of solder exhibits Cu₆Sn₅ and Ag₃Sn phase, no Cu₃Sn was detected, probably due to the low diffusion of Sn, Ag and Cu at fast cooling rates. It indicates that the cooling rate increase the size of the Cu₆Sn₅ phase and inhibited the eutectic network formed in Sn-rich phase. In addition, the grain size of Sn-rich phase of both mold decreased with increased cooling rate. The relation of grain size and cooling condition of casting is discussed in the next section.

Table 1. Results of XRD analyses.

Phase	Crystal Structure	Space group (No.)	Lattice parameters (Å)
Sn	BCT	I41/amd (141)	a = b = 5.8332, c = 3.1820
Ag	FCC	Fm-3m (225)	a = b = c = 4.1280
Cu	FCC	Fm-3m (225)	a = b = c = 3.6150
Cu ₆ Sn ₅	Hexagonal	P63/mmc (194)	a = b = 4.2000, c = 5.0900
Cu ₆ Sn ₅	Monoclinic	C2/c (15)	a = 11.0220, b = 7.2820, c = 9.8270
Ag ₃ Sn	Orthorhombic	Pmmn (59)	a = 5.9680, b = 4.7802, c = 5.1843

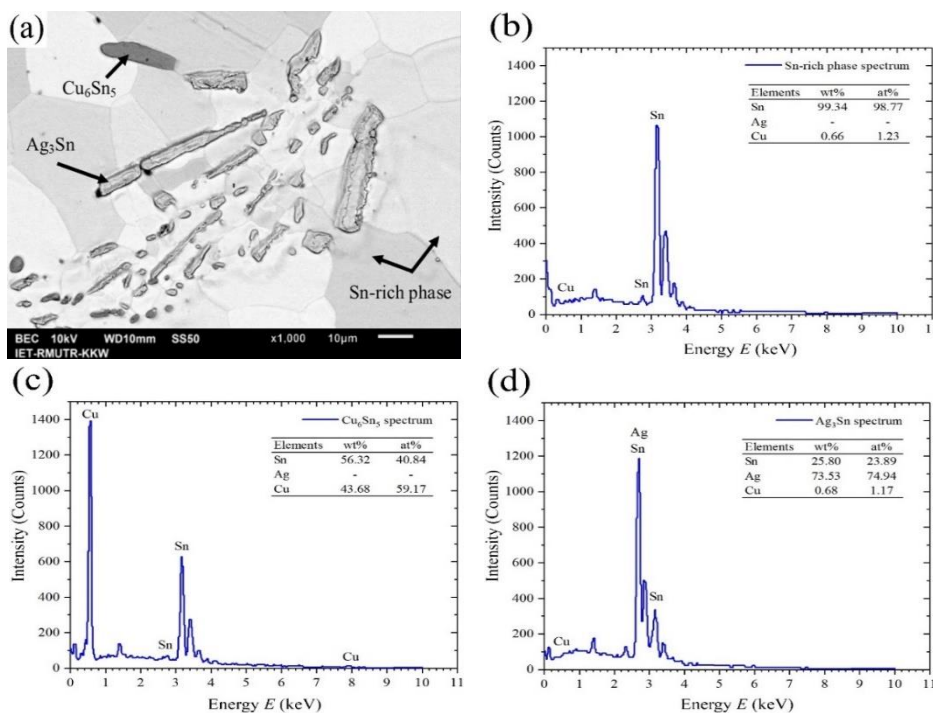


Figure 2. Microstructure and EDS spectrum (a) Microstructure (b) Sn-rich phase, (c) Cu₆Sn₅ and (d) Ag₃Sn.

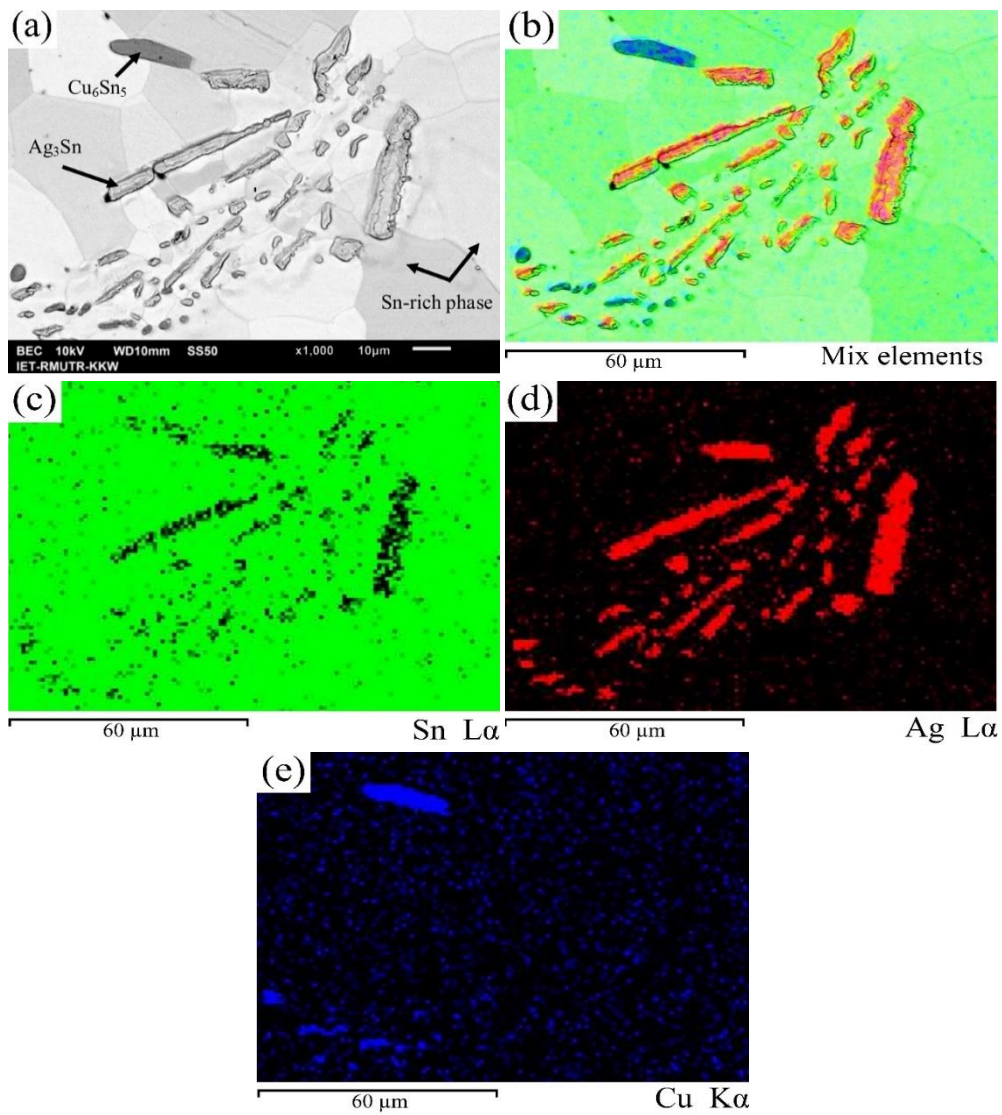


Figure 3. Element maps analyses of solder: (a) SEM micrograph; (b) Mapping of all elements; (c, d, e) Sn (green), Ag (red), Cu (blue) mapping individually.

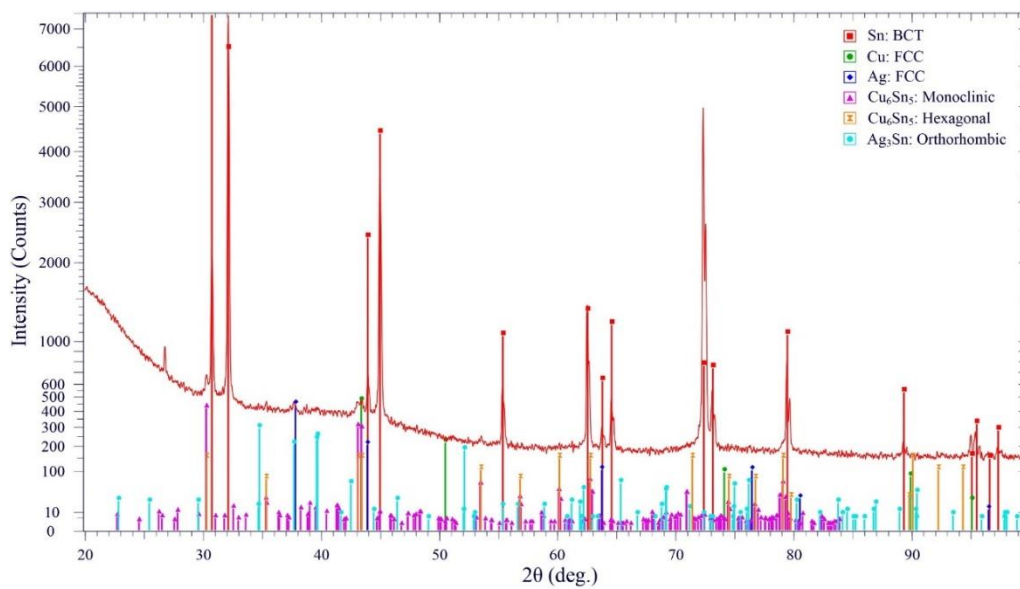


Figure 4. XRD patterns of sample cast with a stainless steel mold and slow cooled.

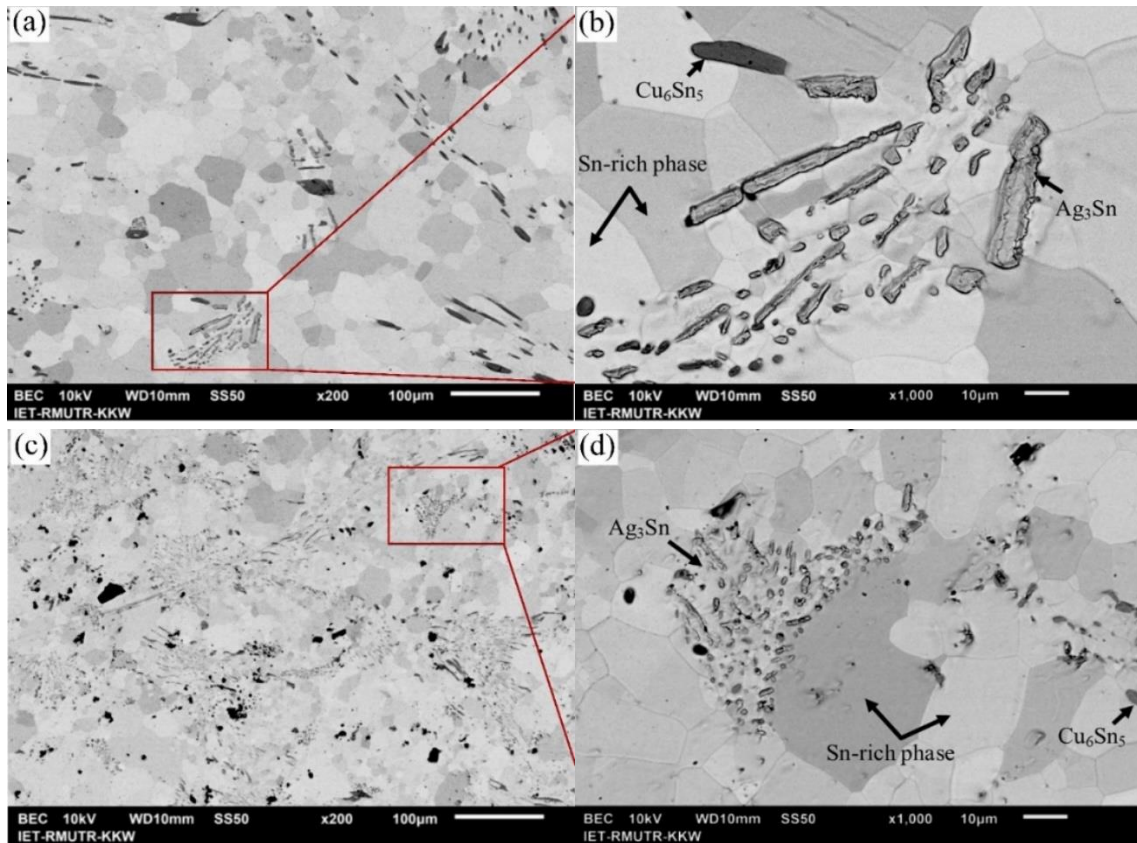


Figure 5. SEM image of samples cast with a copper mold: (a-b) slow cooled and (c-d) fast cooled

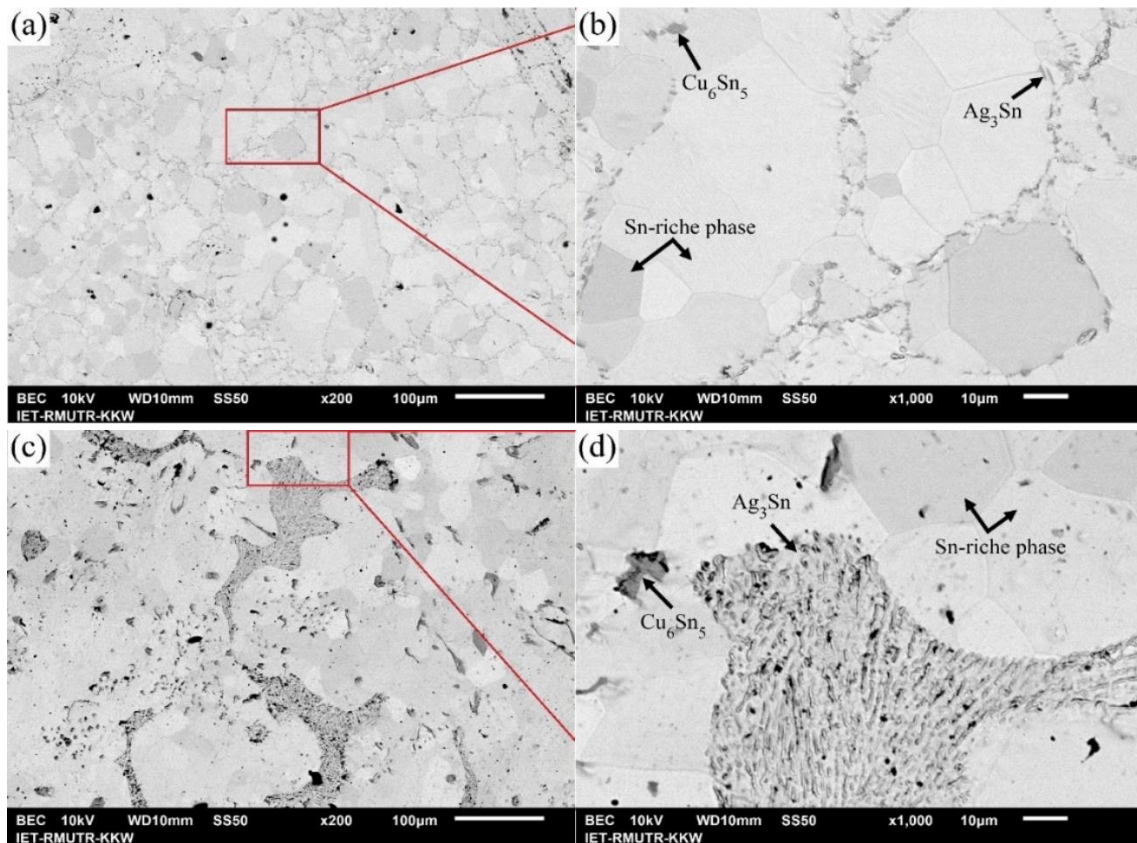


Figure 6. SEM image of samples cast with a stainless steel mold: (a-b) slow cooled and (c-d) fast cooled.

3.1 grain size of Sn-rich phase

The grain size numbers (G) of the Sn-rich phase were determined using the ASTM E112-10 intercept method, as illustrated in Figure 7. The grain size number for structure can be calculated by [22]:

$$G = (6.643856 \log_{10} \bar{P}) - 3.288 \quad (1)$$

Where \bar{P} is the number of grain boundary intersections per unit length.

After solder cooling, it was obvious that the average grain size of Sn-rich phase is increased with the increased cooling rate. The mean grain size numbers were 9.71 and 11.93 by copper mold cast for the slow and fast cooling, respectively. However, the mean grain size number of solder solidified in stainless steel mold was 8.87, and 9.68 for the slow and fast cooling, respectively. The higher value of G represents the smaller grain size.

The influence of mold material on solidification behavior of the microstructure can be explained due to coppers higher thermal conductivity than stainless steel [8]. Thus, microstructure of solder cast in copper mold showed larger grains of Sn-rich phase than when cast in stainless steel mold. In addition, grain size of Sn-rich phase decreases with increasing cooling speed.

In both copper and stainless steel mold, the formation of few IMC particles with Sn-rich phase were coarse grain structures. By fast cooling condition, IMC in the Sn-rich matrix were more distributed than by slow cooling. This was due to the rapid cooling which promoted fine Ag_3Sn particles with spherical morphology dispersed in the Sn-rich matrix [5].

3.2 Mechanical property and fracture behaviors

The tensile strength of the solder was clearly different under the cooling conditions as presented in Figure 8. The tensile strength of sample cast with copper mold was higher than stainless steel for both slow and fast cooling rates. In addition, the tensile strength slightly decreased with the fast cooling rate for both molds. Thus, the higher cooling of the solder alloy contributed to the decrease in tensile strength. This was due to the presence of the higher volume fraction of eutectic area and Ag_3Sn phase. The results of this study resembled those of Guman *et al.* [14]. more Ag_3Sn phase is devaluated the tensile strength. But, dissimilarity with Chellaih *et al.* [8], the formation of Ag_3Sn phase and another type of IMC i.e., Cu_3Sn phase was attributable to an increased tensile strength.

The microhardness of the solder (Figure 9) when slow cooled was consistent with the tensile strength. Meaning the higher strength resulted in the higher microhardness. However, microhardness of the samples with fast cooling rate from both molds was slightly different due to the copper cast solder having more Ag_3Sn distribution in Sn-rich phases which makes it harder.

Fractograph of the solder show all samples exhibited the necking phenomenon and the dimples on the fractured surface as illustrated in Figures 10 and Figure 11 for copper and stainless steel molds, respectively. The size of dimples of fractured surface with copper mold was smaller than the stainless steel mold. The fracture surface of the slow cooled solder exhibited coarse dimples, with the dimples

on the fractured surface confirming the ductile fracture of the fast cooled specimen. Thus, the solder has a low strength and a higher elongation, this was due to the larger eutectic area and Ag_3Sn phase in microstructure of solder alloy

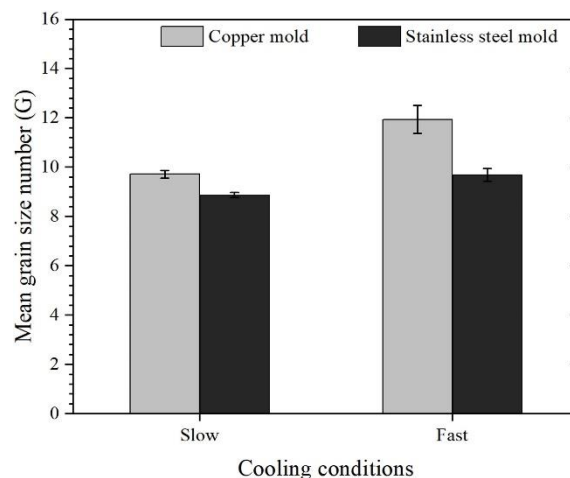


Figure 7. Grain size number of Sn-rich phase with difference condition casting.

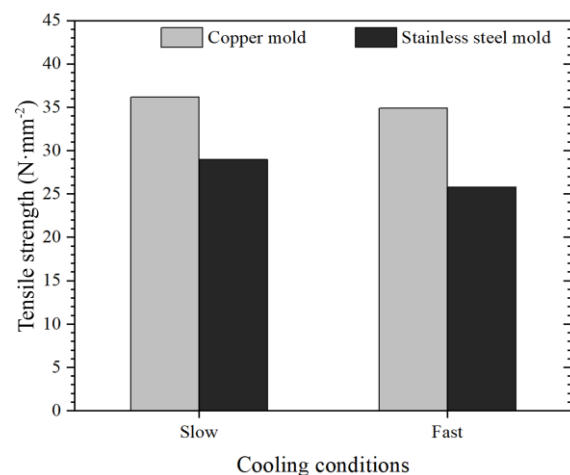


Figure 8. Tensile strength of the solder with difference condition casting.

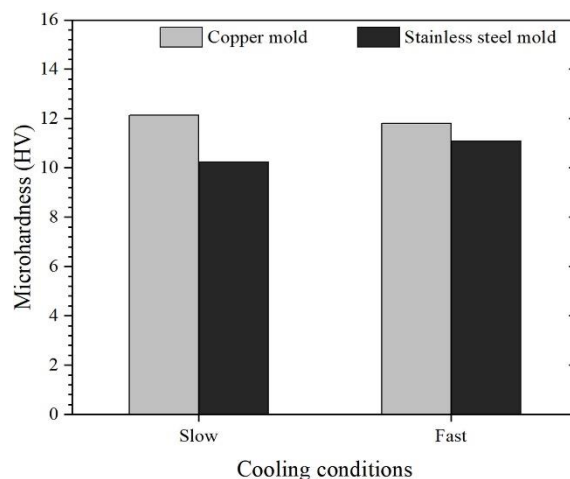


Figure 9. Microhardness of the solder with difference condition casting.

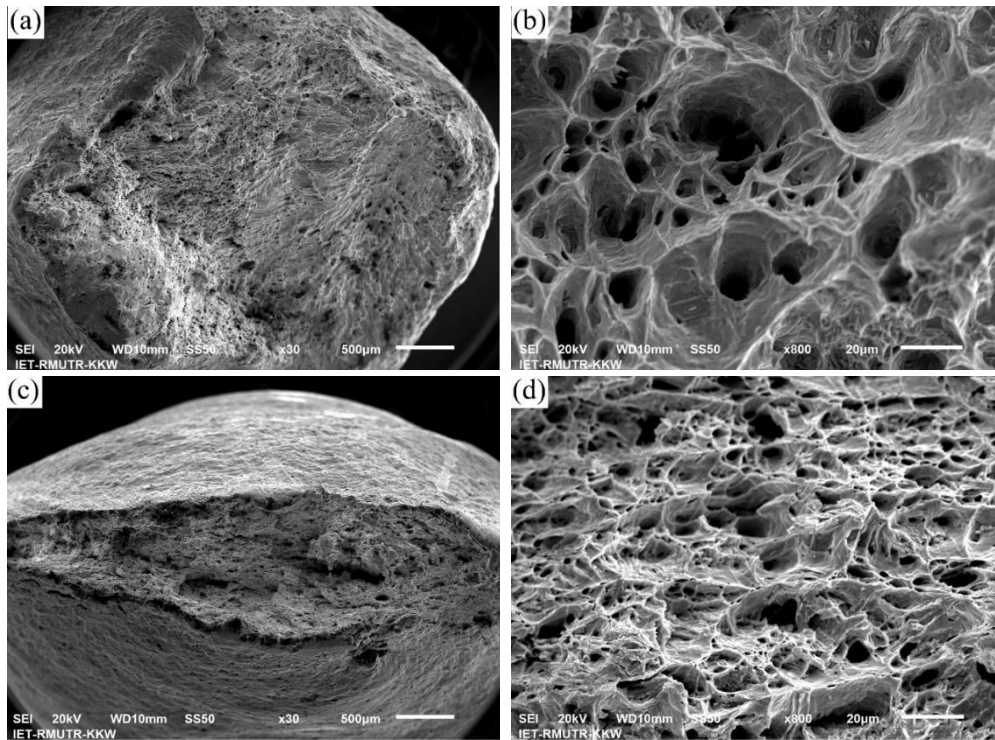


Figure 10. Fractographs of samples with copper mold: (a-b) slow cooled and (c-d) fast cooled.

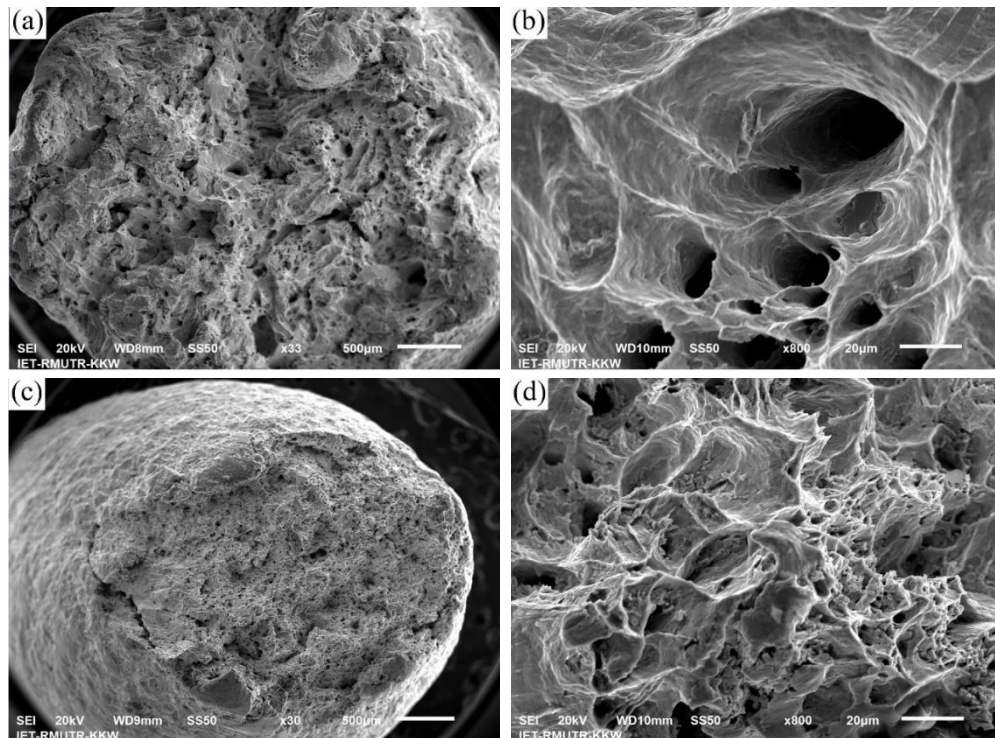


Figure 11. Fractographs of samples with stainless steel mold: (a-b) slow cooled and (c-d) fast cooled.

4. Conclusions

This research examined the influence of cooling conditions on microstructure and mechanical property of Sn-0.3Ag-0.7Cu lead-free solder. To vary the cooling conditions, the solder alloy was cast with copper mold, stainless steel mold, and with slow and fast cooling rates.

It was discovered that the Cu_6Sn_5 and Ag_3Sn intermetallic phases were present in all samples. In addition, Sn-rich phase of solder cast in copper mold showed larger grain size than cast in stainless steel mold. The tensile strength of samples casted with copper mold were greater than the stainless steel mold. However, a faster cooling rate of the solder alloy contributed to decreases the tensile strength and

microhardness properties. The larger eutectic area and Ag₃Sn phase formation in solder alloy presents a lower strength and a higher elongation. It is possible to conclude that the cooling state plays a significant role in the microstructure and mechanical properties of lead-free solder.

Acknowledgements

The authors would like to express sincere gratitude to Rajamangala University of Technology Rattanakosin (RMUTR) for the laboratory support of this project.

Compliance with ethical standards

Conflict of interest The authors declare that they have no conflict of interest

References

- [1] M. Zhao, L. Zhang, Z. Q. Liu, M. Y. Xiong, and L. Sun, "Structure and properties of Sn-Cu lead-free solders in electronics packaging," *Science and Technology of Advanced Materials*, vol. 20, pp. 421-444, 2019.
- [2] L. Gao, S. Xue, L. Zhang, Z. Sheng, F. Ji, W. Dai, S.L. Yu, and G. Zeng, "Effect of alloying elements on properties and microstructures of SnAgCu solders," *Microelectronic Engineering*, vol. 87, pp. 2025-2034, 2010.
- [3] S. Li, X. Wang, Z. Liu, Y. Jiu, S. Zhang, J. Geng, X. Chen, S. Wu, P. He, and W. Long, "Corrosion behavior of Sn-based lead-free solder alloys: a review," *Journal of Materials Science: Materials in Electronics*, vol. 31, pp. 9076-9090, 2020.
- [4] S. N. Alam, P. Mishra, and R. Kumar, "Effect of Ag on Sn-Cu and Sn-Zn lead free solders," *Materials Science- Poland*, vol. 33, pp. 317-330, 2015.
- [5] K. N. Reeve, J. R. Holaday, S. M. Choquette, I. E. Anderson, and C.A. Handwerker, "Advances in Pb-free solder microstructure control and interconnect design," *Journal of Phase Equilibria and Diffusion*, vol. 37, pp. 369-386, 2016.
- [6] J. Powell-Turner, P. D. Antill, and R. E. Fisher, "The United Kingdom Ministry of Defence and the European union's electrical and electronic equipment directives," *Resources Policy*, vol. 49, pp. 422-432, 2016.
- [7] A. Olofinjana, R. Haque, M. Mathir, and N. Y. Voo, "Studies of the solidification characteristics in Sn-Ag-Cu-Bi solder alloys," *Procedia Manufacturing*, vol. 30, pp. 596-603, 2019.
- [8] T. Chellaih, G. Kumar, and K. N. Prabhu, "Effect of thermal contact heat transfer on solidification of Pb-Sn and Pb-free solders," *Materials and Design*, vol. 28, pp. 1006-1011, 2007.
- [9] L. Sun, and L. Zhang, "Properties and microstructures of Sn-Ag-Cu-X lead-free solder joints in electronic packaging," *Advances in Materials Science and Engineering*, Article ID 639028, pp. 1-16, 2015.
- [10] M. Drienovsky, M. Palcut, P. Priputen, E. Cuninková, O. Bošák, M. Kubliha, and L. R. Trnková, "Properties of Sn-Ag-Cu solder joints prepared by induction heating," *Advances in Materials Science and Engineering*, Article ID 1724095, pp. 1-9, 2020.
- [11] P. Manoj Kumar, G. Gergely, D. K. Horváth, and Z. Gácsi, "Investigating the microstructural and mechanical properties of pure lead-free soldering materials (SAC305 & SAC405)," *Powder Metallurgy Progress*, vol. 18, pp. 49-57, 2018.
- [12] P. Roubaud, G. Ng, G. Henshall, and R. Bulwith, "Impact of intermetallic growth on the mechanical strength of Pb-free BGA assemblies," *Proceedings of APEX 2001 on January 16-18, 2001 in San Diego, CA*.
- [13] W. Kittidacha, A. Kanjanavikat, and K. Vattananiyom, "Effect of SAC alloy composition on drop and temp cycle reliability of BGA with NiAu pad finish," *10th Electronics Packaging Technology Conference, EPTC 2008*, pp. 1074-1079, 2008.
- [14] M. S. Gumaan, R. M. Shalaby, E. A. M. Ali, and M. Kamal, "Copper effects in mechanical, thermal and electrical properties of rapidly solidified eutectic Sn-Ag alloy," *Journal of Materials Science: Materials in Electronics*, vol. 29, pp. 8886-8894, 2018.
- [15] J. J. Sundelin, S. T. Nurmi, T. K. Lepistö, and E. O. Ristolainen, "Mechanical and microstructural properties of SnAgCu solder joints," *Materials Science and Engineering A*, vol. 420, pp. 55-62, 2006.
- [16] H. T. Lee and K. C. Huang, "Effects of cooling rate on the microstructure and morphology of Sn-3.0Ag-0.5Cu solder," *Journal of Electronic Materials*, vol. 45, pp. 182-190, 2016.
- [17] M. Z. Yahaya, N. A. Salleh, S. Kheawhom, B. Illes, M. F. Mohd Nazeri, and A. A. Mohamad, "Selective etching and hardness properties of quenched SAC305 solder joints," *Soldering and Surface Mount Technology*, vol. 32, pp. 225-233, 2020.
- [18] K. K. Xu, L. Zhang, L. L. Gao, N. Jiang, L. Zhang, and S. J. Zhong, "Review of microstructure and properties of low temperature lead-free solder in electronic packaging," *Science and Technology of Advanced Materials*, vol. 21, pp. 689-711, 2020.
- [19] R. Pandher, and T. Lawlor, "Effect of silver in common lead-free alloys," *International Conference on Soldering and Reliability, Toronto*, pp. 1-14, 2009.
- [20] K. Kanlayasiri, and T. Ariga, "Influence of thermal aging on microhardness and microstructure of Sn-0.3Ag-0.7Cu-xIn lead-free solders," *Journal of Alloys and Compounds*, vol. 504, pp. L5-L9, 2010.
- [21] C. Wei, Y. C. Liu, Y. J. Han, J. B. Wan, and K. Yang, "Microstructures of eutectic Sn-Ag-Zn solder solidified with different cooling rates," *Journal of Alloys and Compounds*, vol. 464, pp. 301-305, 2008.
- [22] ASTM E112-10, "ASTM International, E112: Standard test methods for determining average grain size," *ASTM International*, vol. 2010, pp. 1-26, 2010.